Evidence for the electron trap state associated with N-rich clusters in InGaAsN/GaAs quantum wells

Evidence for the electron trap state associated with N-rich clusters in InGaAsN/GaAs quantum wells

J F Chen[1], P C Hsieh[1], R S Hsiao[1], J S Wang[2] and J Y Chi[3]

[1] Department of Electrophysics, National Chiao Tung University, Hsinchu, 30010 Taiwan, Republic of China
[2] Department of Physics, Chung Yuan Christian University, Chung-Li, 32023 Taiwan, Republic of China
[3] Industrial Technology Research Institute (OES/ITRI), Hsinchu, 310 Taiwan, Republic of China

E-mail: jfchen@cc.nctu.edu.tw

Abstract
An electron trap state has been found to appear in InGaAsN/GaAs quantum wells (QWs) as a result of composition fluctuation. Evidence of composition fluctuation is shown by photoluminescence spectra which display an additional low-energy emission due to local regions of N-rich clusters. Enhancing composition fluctuation leads to undulated InGaAsN/GaAs interface with dot-like islands. The capacitance–voltage profiling shows an additional peak following the QW electron ground state peak, suggesting the presence of an electron trap state below the QW electron ground state. The emission properties of this trap state are similar to those of quantum dots immersed in a well. Enhancing composition fluctuation can cause an energy downward shift and spectral broadening of this electron trap state, suggesting an increase in island size and fluctuations of the size and composition. Thus, it is deduced that the electron trap state originated from the N-rich clusters in the well behaving like quantum dots. Upon modulation, the electrons are thermally activated from this trap state to the QW electron ground state and subsequently emitted to the GaAs bottom electrode.

1. Introduction

Long wavelength lasers made of InGaAsN/GaAs quantum wells (QWs) are promising for optical fibre communication [1–8]. However, N incorporation often induces recombination centres [9–11] which degrade photoluminescence (PL) efficiency [12, 13]. Increasing growth temperature may alleviate this problem but often leads to composition fluctuation [14–17]. Evidence of composition fluctuation or clustering has been shown by PL spectra [14–18] and transmission electron microscopy (TEM) [17]. Many authors have observed anomalous S-shaped temperature dependence of the emission energy and attributed it to an exciton localization effect due to composition fluctuation [19, 20]. Enhancing composition fluctuation can lead to strong carrier localization and quantum-dot (QD)-like behaviour [21, 22]. Recently, near-field magneto-photoluminescence spectroscopy is used for the estimation of the size, density and depth of these QD-like compositional fluctuations [21, 23, 24]. Despite these achievements, detailed properties of electron emission from these QD states have not been investigated. Understanding this effect is essential not only for physical interest but also for device applications. We have previously shown that lowering the growth rate of the InGaAsN layer degraded PL efficiency and caused electron depletion [25] due to enhanced composition fluctuation. We continue this study by using capacitance–voltage (C–V) profiling and admittance spectroscopy on samples with different degrees of composition fluctuation. Composition fluctuation is shown to induce an electron trap state which can partially trap electrons in the well. Enhancing composition fluctuation can shift downward and broaden the electron trap state. This dot-like behaviour suggests that the electron trap state is induced by N

clusters acting like quantum dots. Possible energy position of the electron trap state and its likely emission process are discussed.

2. Experimental details

The GaAs/InGaAsN/GaAs single-quantum-well (SQW) samples were grown on n^+-GaAs(001) substrates by molecular beam epitaxy equipped with an EPI-Unibulb radio frequency (RF) plasma source to provide nitrogen species from pure N_2 gas. Indium and gallium were supplied from conventional K cells and As in the form of As_2 was supplied from a cracker source. The growth was started with a 0.3 μm Si-doped GaAs layer of $\sim 6 \times 10^{16}$ cm^{-3} grown at 580 °C, followed by a 60 Å-thick InGaAsN layer, grown at 420 °C. To avoid introducing shallow impurities, the InGaAsN layer was undoped. After the growth of the InGaAsN layer, the growth temperature was increased to 580 °C for the growth of a 0.3 μm Si-doped GaAs top layer of $\sim 6 \times 10^{16}$ cm^{-3}. The In and N compositions were obtained from fitting the x-ray diffraction spectra by first determining the In composition from an InGaAs/GaAs SQW structure and then determining the N composition, assuming the In composition remained unchanged. Detailed growth conditions can be found elsewhere [26, 27]. To enhance composition fluctuation, the growth rate of the InGaAsN layer was lowered from 4.4 to 0.5 Å s^{-1} by scaling down the In and Ga fluxes. Due to a difficulty in precisely adjusting the N beam flux, the samples grown at different growth rates may have slightly different N compositions. Schottky contacts were fabricated by evaporating Al with a dot diameter of 800 μm. PL spectra were obtained by a frequency doubled YAG:Nd laser ($\lambda = 532$ nm) and an InGaAs detector.

3. Results and discussions

Lowering the growth rate of the InGaAsN layer enhances composition fluctuations [25]. Figure 1(a) shows the cross section TEM images of the InGaAsN/GaAs SQW samples with the InGaAs layers grown at 4.4, 2.8 and 0.5 Å s^{-1}, respectively. In each sample, the In and Ga compositions are 34% and 66%, respectively. The N composition is 1.6% for the 4.4 Å s^{-1} sample and 2% for 2.8 and 0.5 Å s^{-1} samples. The InGaAsN layer is clearly visible in each sample. A slight degradation of interface sharpness can be seen when lowering the growth rate from 4.4 to 2.8 Å s^{-1}. With a further lowering to 0.5 Å s^{-1}, a rather undulated upper interface with small dark islands can be seen. Reflection high-energy electron diffraction (RHEED) platters turned spotty in this sample, suggesting a transition to three-dimension (3D) growth mode. Similar 3D islands were observed in InGaAsN/GaAs QWs [17] and were attributed to composition fluctuation. To evaluate the optical properties, figure 1(b) shows the PL spectra of the investigated samples under an excitation power of 1.3 mW for the 4.4 Å s^{-1} sample and 325 mW for the 2.8 Å s^{-1} and 0.5 Å s^{-1} samples, respectively. The main peak is related to QW emission. As previously reported [25], lowering the growth rate considerably degrades the QW emission. The wavelength redshift (from 1183 to 1275 nm) from the 4.4 to 2.8 Å s^{-1} sample is due to an increase of N composition from 1.6 to 2%, which also contributes to composition fluctuation. The 2.8 Å s^{-1}
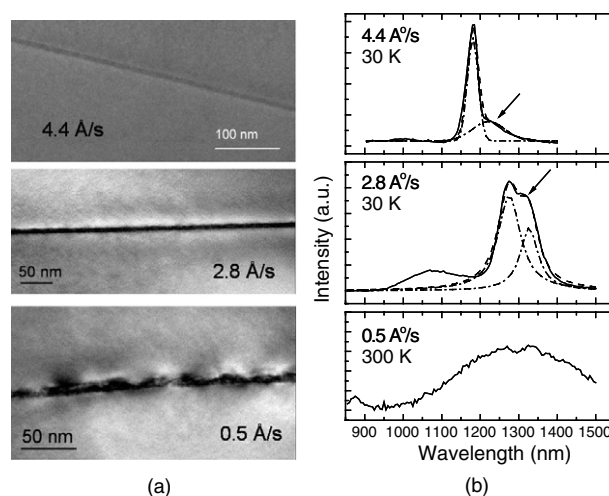

Figure 1. (a) Cross-sectional TEM images of the InGaAsN SQW samples with the InGaAs layer deposited at 4.4 Å s^{-1}, 2.8 Å s^{-1} and 0.5 Å s^{-1}, respectively. Flat interfaces in the 4.4 and 2.8 Å s^{-1} samples and rather undulated interfaces with 3D dark islands in the 0.5 Å s^{-1} sample can be seen. (b) PL spectra of the corresponding samples. Beside the QW emission, a low-energy peak (indicated by arrows) due to composition fluctuation can be seen in the 4.4 and 2.8 Å s^{-1} samples. Further lowering to 0.5 Å s^{-1} severely degrades the PL spectra.

sample displays a broad emission at ~ 1075 nm which is due to recombination of a deep level (detailed properties will be published elsewhere). The spectrum of the 4.4 Å s^{-1} sample displays a low-energy tail (indicated by an arrow). This tail often observed in N–As alloys was attributed to the recombination of excitons trapped by localized states at the band tail induced by composition fluctuation [16]. By fitting the spectrum to two Gaussian curves, this low-energy tail is about 30 meV separated from the QW emission. When composition fluctuation is enhanced by lowering the growth rate to 2.8 Å s^{-1}, this tail becomes a pronounced shoulder with intensity comparable to that of the QW emission. By fitting, this low-energy peak is separated from the QW emission by about 38 meV. The lower emission energy suggests the presence of local regions with N composition higher than the average, i.e. N-rich clusters [16]. With a further lowering to 0.5 Å s^{-1}, the QW emission becomes very weak and broad (centred on 1300 nm). At low temperatures, the spectrum is dominated by the deep-level emission around 1075 nm. These results show an enhancement in composition fluctuation from the 4.4 to 2.8 and to 0.5 Å s^{-1} samples. It should be noted that, in order to retain the composition fluctuation, the studied samples are not annealed after growth. However, considerable improvement of the QW emission and suppression of the N-rich low-energy tail are observed in the 2.8 Å s^{-1} sample after post-growth rapid thermal annealing at 700 °C for 5 min. This result further supports that the low-energy tail is due to composition fluctuation, since annealing is known to effectively alleviate composition fluctuation.

Figure 2 shows the C–V spectra and the corresponding apparent-carrier-concentration profiling of the investigated samples. The concentration peak at ~ 0.3 μm (C–V step at -2 V) is related to the depopulation of the QW electron ground
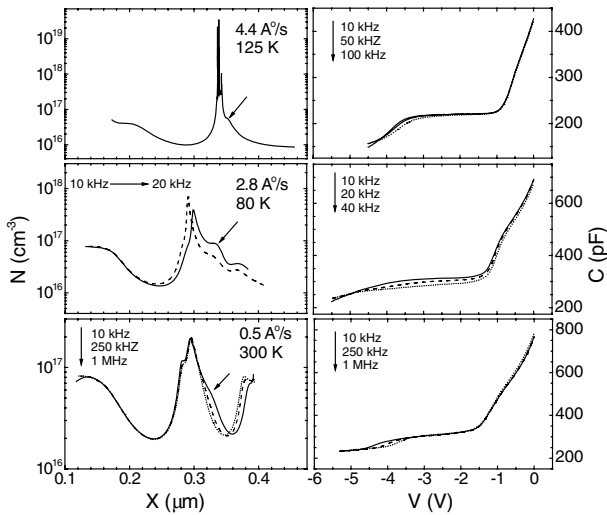
Figure 2. *C–V* spectra and their converted apparent-carrier-concentration profiles of the investigated samples. The *C–V* plateau around −2 V and the corresponding peak around 0.3 μm are due to the discharging of the QW. The additional *C–V* plateau around −4 V and the corresponding peak (indicated by arrows) suggest the presence of an electron trap state below the QW electron ground state. The frequency-dependent dispersions suggest a restively long emission time for this state.

Figure 3. Temperature-dependent *G/F–F* spectra, measured at the dc voltage corresponding to the electron trap state (indicated by arrows in figure 2). Each curve displays a peak at a frequency comparable to the inverse of the emission time. The analysis of *G(F)* and *G(T)* allows us to determine the emission time as a function of temperature.

state (EGS). The peak increases its intensity with lowering temperature, suggesting a Debye-length quantum effect. This peak suffers no frequency-dependent attenuation up to 1 MHz at 10 K, suggesting a very short emission time. The narrowest linewidth in the 4.4 Å s^{-1} sample is consistent with the strongest QW emission. When the dc voltage is decreased to about −4 V, another peak emerges at the right shoulder of the QW peak (indicated by arrows). This indicates the presence of an electron trap state below the QW EGS. The area under the peak is indicative of the density of the state. As shown, this area increases from the 4.4 to 2.8 Å s^{-1} samples, consistent with an enhanced composition fluctuation. Note that this state is not associated with dopant-related shallow impurities since the InGaAsN layer is undoped.

Figure 2 shows frequency-dependent attenuation for the right-shoulder carrier peak, suggesting an observable electron emission time for the trap state. The emission time is investigated by means of admittance spectroscopy [25]. Figure 3 shows the conductance/frequency–frequency (*G/F–F*) spectra, measured at the dc bias corresponding to the right-shoulder carrier peak. Each sample displays a peak at a frequency comparable to the inverse of the emission time. Figure 4 shows the Arrhenius plots of their emission times from which we obtain an activation energy (capture cross section) of 32 ± 24 meV (1.3 × 10^{-18} cm^2) for the 4.4 Å s^{-1} sample. The activation energy (capture cross section) of the 2.8 Å s^{-1} sample shows a slightly dc bias dependence, which increases from 88 (5.2 × 10^{-18} cm^2) to 94 meV (2.7 × 10^{-17} cm^2) from −3 to −4.5 V. Beyond −4.5 V, the conductance peak rapidly diminishes due to the emptying of electrons in the trap state and no reliable data could be obtained. In view of the close proximity between the right-shoulder carrier peak and the QW peak (in figure 2), we place the electron state at the obtained acti-
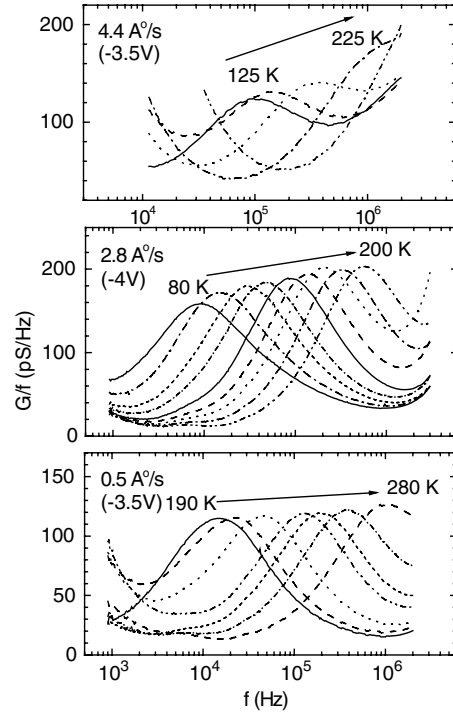
vation energy below the QW EGS as shown in the electronic structure in figure 5, where the conduction-band band offset is estimated to be ∼0.3 eV [18, 29] from the QW emission energy. Upon modulation, we speculate that electrons are thermally activated from the electron state to the QW EGS and subsequently activated to the bottom GaAs electrode. The short emission time for the latter process was not resolved, as there was no frequency-dependent attenuation in the QW peak up to 1 MHz at 10 K.

The admittance spectroscopy indicates that the energy difference between the electron state and the QW EGS is 32 meV in the 4.4 Å s^{-1} sample which increases to ∼88 meV in the 2.8 Å s^{-1} sample. These values are comparable with the energy spacing (30–38 meV) between the PL low-energy tail and the QW emission (in figure 1(b)), strongly suggesting that the electron state causes the low-energy PL emission. This correlation is further supported by the fact that both are observed at low temperatures and simultaneous enhancement in the right-shoulder carrier peak and the low-energy PL emission from the 4.4 to 2.8 Å s^{-1} samples. It should be noted that our observed energy spacing of 30–38 meV is comparable to the previously observed localization energy of 10–60 meV observed between the QW emission (Varshni's model) and sharp emission lines due to composition fluctuation by near-field magneto-PL spectroscopy [21]. This comparability further supports that the low-energy emissions are caused by composition fluctuation.

As to the 0.5 Å s^{-1} sample, the Arrhenius plots in figure 4 yield an activation energy (capture cross section) of 0.11 eV
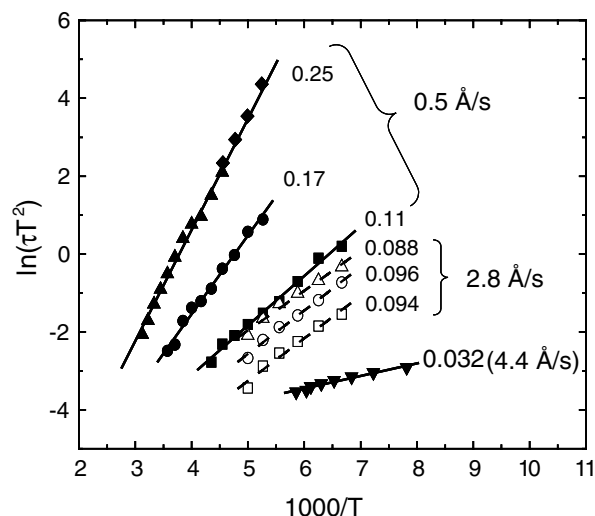
Figure 4. Arrhenius plots of the emission times of the electron trap states under various dc voltages for the investigated samples. Activation energies of 0.032, 0.088 to 0.096, and 0.11 to 0.25 eV are determined for the 4.4, 2.8 and 0.5 Å s^{-1} samples, respectively.
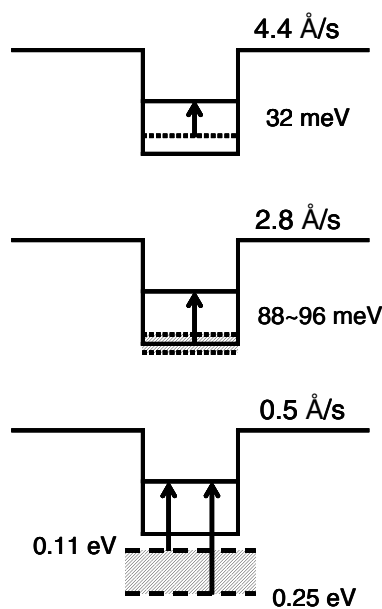

Figure 5. Schematic conduction-band diagrams of the SQW samples, illustrating the energy position of the electron trap state (the horizontal dashed lines) and the QW electron ground state (the horizontal solid line) as composition fluctuation is enhanced from the 4.4 to 2.8 and to the 0.5 Å s^{-1} samples.

$(1.6 \times 10^{-17}$ cm$^2)$ for a dc bias of -3 V, which continuously increases to 0.25 eV $(2.2 \times 10^{-16}$ cm$^2)$ for -4 V. Beyond this range, the conductance peak is so small that no reliable data could be obtained. This relatively large activation energy gives rise to a long emission time, leading to the appearance of the frequency dispersion of the right-shoulder carrier peak around 300 K (in figure 2). The trend of increasing activation energy contradicts the effect of tunnelling since a large reverse bias would increase tunnelling probability and reduce activation energy. Thus, it is explained by a broadening of the electron

state into a continuum of states from 0.11 to 0.25 eV. As in the 4.4 and 2.8 Å s^{-1} samples, we place the continuum of the states at the obtained activation energies below the QW EGS. These results show an energy downward shift and spectral broadening of the electron trap state by enhancing composition fluctuation.

As shown in figure 1(a), the TEM image shows dot-like islands in the 0.5 Å s^{-1} sample. If these islands can trap electrons, upon modulation, the trapped electrons can emit from these islands to the GaAs bottom electrode, leading to the emergence of the right-shoulder carrier peak. The energy downward shift suggests an increase in the island size as a result of enhanced composition fluctuation, and the spectral broadening suggests the fluctuation of island size, composition and shape. This indicates a dot-like behaviour [28] for the electron state. Given this trend, it is plausible that the 4.4 and 2.8 Å s^{-1} samples also contain islands (N clusters) although the size may be relatively small.

Finally, one may raise a question about another possible origin for the electron state; that is, it is not induced by composition fluctuation but is an impurity or point defect whose emission properties are affected by composition fluctuation. Composition fluctuation can cause locally different bandgaps. Electron emission from the trap to such a band edge would have fluctuation of activation energy as the spectral broadening. However, the trend of the energy downward shift cannot be explained. A defect trap is believed to have a quite localized wavefunction for a trapped electron. If composition fluctuation only affects the neighbouring atoms surrounding the trap, the downward shift is expected to be small with respect to the downward shift of the InGaAsN conduction-band edge when N composition is increased. As a result, when N composition is increased from 1.6 to 2% (from the 4.4 to 2.8 Å s^{-1} samples), one would expect a decrease in the activation energy of the trap, instead of an increase as observed. In other words, an impurity or point defect is unlikely to increase its activation energy when the bandgap of the host material is reduced. Furthermore, the comparative analysis of the PL and C–V profiling demonstrates a close correlation between the electron trap state and the low-energy PL emission. Hence, we believe that degraded composition fluctuation can form N-rich clusters in the well acting like quantum dots.

4. Conclusions

In summary, an electron trap state induced by composition fluctuation is analysed in InGaAsN/GaAs single quantum wells. An additional low-energy PL emission and undulated interfaces with dot-like islands suggest the presence of local regions of N-rich clusters. Apparent-carrier-concentration profiling shows an additional carrier-confinement peak, suggesting the presence of an electron trap state below the QW electron ground state. When composition fluctuation is enhanced, this electron state shifts downward and broadens. These features are similar as those observed in quantum dots, suggesting that the electron state originates from N-rich clusters acting like dots. The results of the present studies also suggest a way to evaluate clustering by analysing its electron trapping.

Acknowledgments

References

[1] Kondow M, Uomi K, Niwa A, Kitatani T, Watahiki S and Yazawa Y 1996 *Japan. J. Appl. Phys.* **35** 1273

[2] Hohnsdorf F, Koch J, Agert C and Stolz W 1998 *J. Cryst. Growth* **195** 391

[3] Wagner A, Ellmers C, Hohnsdorf F, Koch J, Agert C, Leu S, Hofmann M, Stolz W and Ruhle W W 2000 *Appl. Phys. Lett.* **76** 271

[4] Sato S, Osawa Y, Saitoh T and Fujimura I 1997 *Electron. Lett.* **33** 1386

[5] Kondow M, Nakatsuka S, Kitatani T, Yazawa Y and Kai M 1996 *Japan. J. Appl. Phys.* **35** 5711

[6] Nakahara K, Kondow M, Kitani T, Larson M C and Uomi K 1998 *IEEE Photon. Technol. Lett.* **10** 487

[7] Weyers M, Sato M and Ando H 1992 *Japan. J. Appl. Phys.* **31** 853

[8] Sato S, Osawa Y and Saitoh T 1997 *Japan. J. Appl. Phys.* **36** 2671

[9] Kwon D, Kaplar R J, Ringel S A, Allerma A A, Kurtz S R and Jones E D 1999 *Appl. Phys. Lett.* **74** 2830

[10] Krispin P, Spruytte S G, Harris J S and Ploog K H 2000 *J. Appl. Phys.* **88** 4153

[11] Kaplar R J, Ringel S A, Kurtz S R, Klem J F and Allerman A A 2002 *Appl. Phys. Lett.* **80** 4777

[12] Xin H P and Tu C W 1998 *Appl. Phys. Lett.* **72** 2442

[13] Kurtz S R, Allerman A A, Jones E D, Gee J M, Banas J J and Hammons B E 1999 *Appl. Phys. Lett.* **74** 729

[14] Spruytte S G, Coldren C W, Harris J S, Krispin P, Ploog K and Larson M C 2001 *J. Appl. Phys.* **89** 4401

[15] Pinault M A and Tournie E 2001 *Appl. Phys. Lett.* **79** 3404

[16] Buyanova I A, Chen W M, Pozina G, Bergman J P, Monemar B, Xin H P and Tu C W 1999 *Appl. Phys. Lett.* **75** 501

[17] Xin H P, Kavanagh K L, Zhu Z Q and Tu C W 1999 *Appl. Phys. Lett.* **74** 2337

[18] Pan Z, Li L H, Lin Y W, Sun B Q, Jiang D S and Ge W K 2001 *Appl. Phys. Lett.* **78** 2217

[19] Grenouillet L, Bru-Chevallier C, Guillot G, Gilet P, Duvaut P, Vannuffel C, Million A and Chenevas-Paule A 2000 *Appl. Phys. Lett.* **76** 2241

[20] Sun H D, Hetterich M, Dawson M D, Egorov A Yu, Bernklau D and Riechert H 2002 *J. Appl. Phys.* **92** 1380

[21] Mintairov A M, Kosel T H, Merz J L, Blagnov P A, Vlasov A S, Ustinov V M and Cook R E 2001 *Phys. Rev. Lett.* **87** 277401

[22] Sun H D, Clark A H, Calvez S, Dawson M D, Gilet P, Grenouillet L and Million A 2005 *J. Appl. Phys.* **97** 033517

[23] Merz J L, Mintairov A M, Kosel T and Sun K 2004 *IEE Proc. Optoelectron.* **151** 346

[24] Mintairov A M, Blagnov P A, Merz J L, Ustinov V M, Vlasov A S, Kovsh A R, Wang J S, Wei L and Chi J Y 2004 *Physica* E **21** 385

[25] Chen J F, Hsiao R S, Hsieh P C, Wang J S and Chi J Y 2006 *J. Appl. Phys.* **99** 123718

[26] Hsiao R S *et al* 2004 *Japan. J. Appl. Phys.* **43** L1555

[27] Wang J S, Kovsh A R, Hsiao R S, Chen L P, Chen J F, Lay T S and Chi J Y 2004 *J. Cryst. Growth* **262** 84

[28] Chen J F, Hsiao R S, Wang C K, Wang J S and Chi J Y 2005 *J. Appl. Phys.* **98** 013716

[29] Carrere H, Marie X, Barrau J, Amand T, Ben Bouzid S, Sallet V and Harmand J-C 2004 *J. Phys.: Condens. Matter* **16** S3215